

Freestyle Sketch-in-the-Loop Image Segmentation

Subhadeep Koley^{1,2} Viswanatha Reddy Gajjala* Aneeshan Sain¹ Pinaki Nath Chowdhury¹

Tao Xiang^{1,2} Ayan Kumar Bhunia¹ Yi-Zhe Song^{1,2}

¹SketchX, CVSSP, University of Surrey, United Kingdom.

²iFlyTek-Surrey Joint Research Centre on Artificial Intelligence.

{s.koley, a.sain, p.chowdhury, t.xiang, a.bhunias, y.song}@surrey.ac.uk

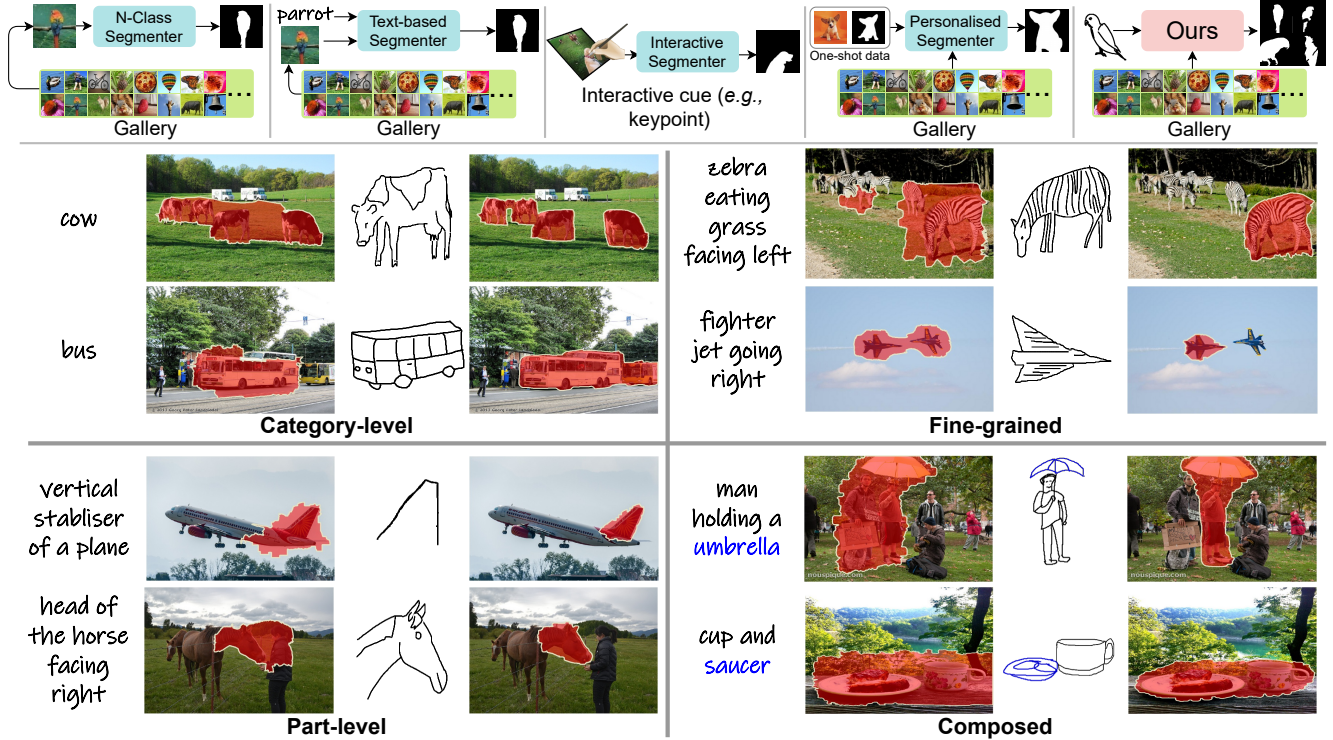


Figure 1. (Top:) Existing deep-learning based image segmentation pipelines can be divided into four categories – (i) Generic N -class segmentation models [49] segment images from a fixed gallery set, (ii) Query-based models [39, 51] segment images with additional inputs (e.g., class-labels, text, etc.), (iii) Interactive models [17, 28] ask users to locate/draw background and foreground cues (e.g., keypoints) for segmentation, and (iv) Personalised models [91] customise large-scale pre-trained segmentation models [39] with a few labelled examples to learn to segment a particular concept. Contrarily, our method can segment all instances of a visual concept present in a gallery with a single exemplar sketch. (Bottom:) Comparison of a few segmented images by our method with a text-based segmenter. Utilisation of sketch enables segmentation at multiple granularity levels (e.g., category-level, fine-grained, part-level). While writing granularity-specific textual cues is cumbersome and difficult, with simple freehand sketches, the proposed method segments either “all” cows (i.e., category-level), “that” zebra (i.e., fine-grained), “head” of the horse (i.e., part-aware), or even composed concepts like a “cup” and a “saucer”.

Abstract

In this paper, we expand the domain of sketch research into the field of image segmentation, aiming to establish freehand sketches as a query modality for subjective image segmentation. Our innovative approach introduces a “sketch-in-the-loop” image segmentation framework, enabling the segmentation of visual concepts partially, completely, or in groupings – a truly “freestyle” approach – without the need for a purpose-made dataset (i.e., mask-free). This framework capitalises on the synergy between sketch-based image retrieval (SBIR) models and large-scale

pre-trained models (CLIP or DINOv2). The former provides an effective training signal, while fine-tuned versions of the latter execute the subjective segmentation. Additionally, our purpose-made augmentation strategy enhances the versatility of our sketch-guided mask generation, allowing segmentation at multiple granularity levels. Extensive evaluations across diverse benchmark datasets underscore the superior performance of our method in comparison to existing approaches across various evaluation scenarios.

1. Introduction

This paper delves into the realm of image segmentation, but with a unique twist – the incorporation of freehand sketches.

*Interned with SketchX

Our research vision is to explore the impact of fine-grained subjectivity inherently captured by a sketch [19, 30], on image segmentation. At its core, our aim is to devise a *subjective* image segmentation framework that empowers users to freely segment any object, be it a partial segment, a complete entity, or a group of interconnected elements – essentially, enabling image segmentation in a “freestyle” manner.

Image segmentation has witnessed significant evolution [14, 39] over time, and we are committed to keeping pace with the current capabilities of image segmentation systems – we also want to operate in an open-vocabulary [57] manner and harness the potential of the latest foundation models. We too fully acknowledge prior segmentation methods that inject subjectivity through textual inputs [85]. The central argument of this paper however revolves around the premise that sketches offer a more precise form of subjectivity – a point convincingly illustrated in Fig. 1 (bottom).

To elucidate why sketches serve as a superior modality for capturing subjectivity, we direct readers to the extensive sketch literature [10, 19, 25, 74, 86]. In summary, the insights drawn from this large body of work are two-fold: (i) sketches excel in their ability to convey intricate visual details that may be cumbersome or ambiguous when expressed through text [74]. (ii) sketches exhibit a smaller semantic gap to photos, as both share the same visual modality, albeit in an abstract form [30]. This inherent relationship is notably featured in the extensively studied domain of SBIR [20] and its fine-grained variations [7] – a challenge that we also employ as a guiding critic in our training.

The specifics of our vision present significant challenges. First and foremost, we need to operate without any sketch-mask pairing data. The collection of such a dataset is simply unfeasible, especially considering the current status quo within the sketch community still concerns gathering enough sketch-photo pairs [58, 73], let alone pixel-perfect masks. This challenge is further exacerbated by our open-vocabulary setting, which essentially renders prior arts inapplicable [31]. Secondly, akin to most prior work in the sketch literature [6, 41, 72, 86], we face a substantial gap between the sketch and photo domains.

We commence by fixating on the ultimate goal: given a sketch, compute corresponding segmentation masks for *all* applicable gallery photos. Surprisingly, it turns out that all we need to compute this correspondence is the strategic utilisation of (i) a frozen Fine-Grained Sketch-Based Image Retrieval (FG-SBIR) model and (ii) a pre-trained foundation model (e.g., CLIP [68], DINOv2 [60]). The former provides a solid foundation for fine-grained sketch-photo correspondence and also serves as a training signal to fine-tune the latter. Meanwhile, the fine-tuned version of the latter predicts the actual mask for the photo using its corresponding sketch, thereby eliminating the need for manually annotated masks (i.e., mask-free). It follows that these two

components are intricately linked by this very hypothesis: a sketch and its matching background-masked image pair (and foreground highlighted) will sit closely within the fixed FG-SBIR joint embedding [72]. This, we hope, is intuitive – the *more highlighted* (using the computed mask) the foreground object is, the *easier* it is for its matching sketch to locate. It is through this iterative training process that the segmentation model continually hones its performance.

In generating sketch-guided masks, we use pre-trained DINOv2 [60] for the fine-grained setup (CLIP [68] for category-level). It extracts a spatial feature map from a photo and a global feature vector from a sketch. A cosine similarity computation, followed by bilinear upscaling and differentiable thresholding, yields a pseudo mask used for generating the background-masked image corresponding to the given sketch. To prevent *all-white* mask predictions and overfitting, a mask-regularisation loss is introduced. Additionally, for part-level segmentation, we employ sketch-partitioning, randomly fragmenting binary sketches into orthogonal splits, enabling model-prediction from a specific split, for more precise part-level segmentation.

In summary, our contributions are (i) we address the challenge of subjective segmentation by introducing a novel approach that enables mask-free image segmentation through the interpretive power of sketches. (ii) we support multi-granularity segmentation, providing users with the flexibility to segment visual concepts at various levels, encompassing entire entities, specific parts, or interconnected groups. (iii) we establish an effective synergy between sketch-based image retrieval models and large-scale pre-trained models. (iv) we propose a purpose-made augmentation strategy that enhances the framework’s versatility, enabling segmentation at multiple granularity levels.

2. Related Works

Sketch for Vision Tasks. *Freehand sketches* has long established its significance for several visual understanding tasks [8, 10, 19, 41, 72, 86]. Following its success in 2D and 3D image retrieval [24, 53, 54, 72, 86], *sketch* as a vision-modality has been used in image generation [41], saliency detection [10], inpainting [87], shape-modelling [56], augmented reality [54], medical image analysis [40], image editing [47, 90], object detection [19], representation learning [22], class-incremental learning [8], etc. To our best knowledge, Sketch-a-Segmenter [31] is the only existing work dealing with sketch-guided segmentation. This method [31] however requires fully-annotated pixel-level masks for training [31], unlike ours. We thus here aim to forward sketch research in another interesting direction by utilising its potential as a weak label for segmentation.

Segmentation in Vision. Image segmentation [14, 15, 49, 70] can be broadly classified into three categories based on *task granularity* – (i) *semantic* segmentation [49, 81, 93] – aims to classify and label each pixel into a set of pre-defined

classes, (ii) *instance* segmentation [29, 77] – involves identifying different *instances* of each object, (iii) *panoptic* segmentation [35, 84] – combines semantic and instance segmentation to simultaneously assign class labels and identify object instances. Rising popularity of vision-language [68] and generative [36, 69] models further inspired *open-vocab* segmentation frameworks like GroupViT [83], Seg-CLIP [52], Segmentation-in-Style [61], ODISE [84], etc. The recent Segment Anything Model (SAM) [39] introduces a zero-shot framework capable of handling diverse segmentation tasks in different image distributions [39]. Its success promoted multiple follow-up works like HQ-SAM [37], PerSAM [91], etc. Our aim here is to introduce the subjectivity of freehand sketches for image segmentation. Moreover, unlike prior methods, our approach segments *all* similar instances of the query sketch from a large gallery of photos instead of segmenting a single image at hand.

Weakly/Un-Supervised Segmentation. Weakly supervised frameworks typically use image-level labels [4, 45, 65–67], scribbles [46, 79], bounding-boxes [21, 38, 63], cue points [5], eye-tracking data [62], web-tags [2], saliency masks [59], etc. as a source for weak-supervision. Such methods can be broadly classified as – (i) *one* stage and (ii) *two* stage. While one-stage methods [4, 13, 63, 66] directly use image-level labels for training, they tend to perform lower than two-stage ones, which first generate pseudo segmentation labels via attention maps [76, 94] and then use them for training. In contrast, unsupervised image segmentation can be broadly divided into two categories– (i) *generative methods* utilise unlabelled images to train specialised image generators [3, 16] or use pre-trained generators to directly generate segmentation masks [1, 55, 80]; (ii) *discriminative methods* are mainly based on clustering and contrastive learning [34, 78, 82, 92].

3. Revisiting Sketch-based Image Retrieval

Here we revisit the baseline SBIR paradigms in favour of the broader vision community. Baseline *category-level* [20] and *fine-grained* [72] SBIR models described here will be used later (Sec. 4.3) to guide the training of our *mask-free* sketch-based *category-level* and *fine-grained* image segmentation models respectively.

Baseline Category-level SBIR. Provided a query sketch $\mathcal{S} \in \mathbb{R}^{H \times W \times 3}$ of any class, category-level SBIR aims to retrieve a photo p_i^j from the *same* class, out of a gallery $\mathcal{G} = \{p_i^j\}_{i=1}^{N_j} |_{j=1}^{N_c}$ containing images from a total N_c classes with N_j images per class [72]. Particularly, a backbone feature extractor (*separate* weights for sketch and photo branches) network is trained to generate d -dimensional feature vector $f_i = \mathcal{F}(\mathcal{I}) : \mathbb{R}^{H \times W \times 3} \rightarrow \mathbb{R}^d$ via triplet loss [88] that aims to minimise the distance $\delta(a, b) = \|a - b\|_2$ between an anchor sketch (\mathcal{S}) feature f_s and a positive photo (\mathcal{P}) feature f_p from the same category as \mathcal{S} , while

increasing that from a negative photo (\mathcal{N}) feature f_n of a different category. With margin $\mu_{\text{cat}} > 0$, triplet loss for category-level SBIR could be formulated as: $\mathcal{L}_{\text{triplet}}^{\text{cat}} = \max\{0, \mu_{\text{cat}} + \delta(f_s, f_p) - \delta(f_s, f_n)\}$

Baseline Fine-grained (FG) SBIR. Unlike category-level, *cross-category FG-SBIR* setup intends to learn a single model capable of fine-grained instance-level matching from multiple (N_c) classes. Akin to category-level [72], cross-category FG-SBIR framework learns a backbone feature extractor $\mathcal{F}(\cdot)$ (weights *shared* between sketch and photo branches), via triplet loss $\mathcal{L}_{\text{triplet}}^{\text{fine}}$ (similar to $\mathcal{L}_{\text{triplet}}^{\text{cat}}$) but with *hard* triplets, where the negative sample is a *different instance* ($\mathcal{P}_k^j; k \neq i$) of the *same class* as the anchor sketch (\mathcal{S}_i^j) and its matching photo (\mathcal{P}_i^j) [72]. Furthermore, for learning inter-class discrimination, it uses an N_c -class classification head with cross-entropy loss ($\mathcal{L}_{\text{class}}$) on the sketch-photo joint embedding space. Thus, the total loss [9] for baseline FG-SBIR is: $\mathcal{L}_{\text{triplet}}^{\text{fine}} + \mathcal{L}_{\text{class}}$.

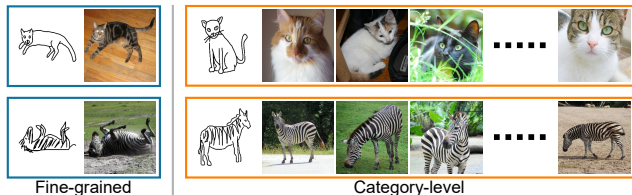


Figure 2. Examples of *fine-grained* (left) and *category-level* (right) image pairs from Sketchy [73] dataset.

Datasets. Category-level datasets like Sketchy-Extended [48, 73], TU-Berlin [26], Quick!, Draw [27], etc. hold category-level association, where *every* sketch of a category is associated with *all* photos of the *same* category as $\{s_i^j, \{p_k^j\}_{k=1}^{N_j^P}\}_{i=1}^{N_j^S} |_{j=1}^{N_c}$ from N_c classes with every j^{th} class having N_j^S sketches and N_j^P photos. Whereas, FG-SBIR datasets (*e.g.*, Sketchy [73]) contain instance-level sketch-photo pairs as $\{s_i^j, p_i^j\}_{i=1}^{N_j} |_{j=1}^{N_c}$ from N_c classes with every j^{th} class having N_j sketch-photo pairs with *fine-grained association*. Here we use category-level and fine-grained SBIR models [71] trained with Sketchy-Extended [73] and Sketchy [73] datasets respectively.

4. Proposed Methodology

Overview. Given an image $\mathcal{I} \in \mathbb{R}^{h \times w \times 3}$, state-of-the-art supervised image segmentation models [14, 15, 49] aim to generate a segmentation mask $\mathcal{M} \in \mathbb{R}^{h \times w \times (c+1)}$ via pixel-level classification across a pre-defined set of c classes and a background (+1). On the contrary, given a query sketch \mathcal{S} , our method generates a binary segmentation mask $\mathcal{M} \in \mathbb{R}^{h \times w \times 1}$, depicting the pixel-locations, wherever the *queried-concept* appears in *any* candidate image $\mathcal{I} \in \mathbb{R}^{h \times w \times 3}$, with pixels belonging to that concept marked as 1 and all the rest as 0. Learning segmentation frameworks via typical supervised training setup however, is impractical given the laborious process of collect-

ing human-annotated ground truth segmentation masks. We therefore aim to utilise the existing sketch-photo dataset [73] to devise a weakly-supervised mask-free image segmenter. Although existing weak supervision signals (query) like tags [2], caption [57], cue points [5], etc. might suffice for category-level vision tasks, they lack in fine-grained cues unlike sketches [10, 19]. Inspired by *sketch*’s success in multiple fine-grained vision tasks (e.g., retrieval [72], detection [19], generation [41], etc.), we aim to establish *sketch* as a worthy query-modality for *mask-free* weakly-supervised image segmentation, both at *category-level* and *fine-grained* setup. Furthermore, we also extend our method to *part-level* segmentation, using the same dataset.

4.1. Problem Definition: Segmentation Granularity

Category Level Segmentation. In this setup, we aim to predict a binary segmentation mask, denoted as $\mathcal{M} \in \mathbb{R}^{h \times w \times 1}$, based on a query sketch \mathcal{S}_c for a specific category, denoted as c . \mathcal{M} will distinguish the foreground object (of category c) by marking the pixels inside the boundary as 1, while the background pixels are set to 0. Essentially, when you draw a “camel” this system will generate segmentation masks for any “camel” photos in the *entire* test gallery.

Fine-grained Segmentation. Given a query sketch \mathcal{S}_f depicting a specific *object instance* of category c , we generate similar segmentation masks $\mathcal{M} \in \mathbb{R}^{h \times w \times 1}$ for any photo in the gallery of category c where the object holds the *same shape/pose* as that of \mathcal{S}_f . For instance, drawing a “camel sitting down” should generate masks *only* for those photos where the camel(s) is(are) “sitting down” in the *same shape/pose*, not *any* photo containing “camel” (Fig. 3 (left)).

Part-level Segmentation. Unlike existing weak supervision signals (e.g., tags [2], cue points [5], etc.), sketch has the ability to model *part-level query* [32]. Accordingly, given a query sketch \mathcal{S}_p depicting a *specific part* of an object from category c , the aim is to generate similar segmentation masks $\mathcal{M} \in \mathbb{R}^{h \times w \times 1}$ depicting *only the queried part* for any photo in \mathcal{G} of category c . For instance, drawing “a camel’s head” should generate segmentation masks showing only the “head” for *any* “camel” photos in \mathcal{G} (Fig. 3 (right)). Here the part-level query \mathcal{S}_p is a region-wise *spatial-subset* ($\mathcal{S}_p \subset \mathcal{S}$) of the full query \mathcal{S} .



Figure 3. *Fine-grained* (left) and *part-level* (right) segmentation.

4.2. Baseline Weakly Supervised Segmentation

In our setup, we consider the available sketches (\mathcal{S}) and photos (\mathcal{P}) from $\mathcal{D}_{\text{cat}} = \{\mathcal{S}_i, \mathcal{P}_i\}_{i=1}^M$ and $\mathcal{D}_{\text{fine}} = \{\mathcal{S}_j, \mathcal{P}_j\}_{j=1}^N$ with category-level [48] and fine-grained [73] association between them respectively (cf. Sec. 3). We design our baseline sketch-based image segmenter taking inspiration from text-based weakly-supervised segmentation framework [57] that employs patch-wise InfoNCE loss between CLIP’s

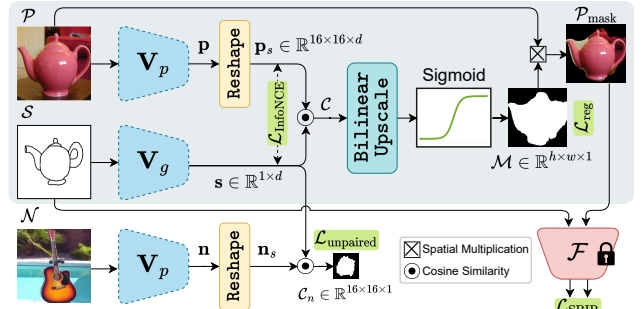


Figure 4. We generate sketch-guided correlation map \mathcal{C} by multiplying the *global* sketch feature \mathbf{s} with reshaped *patch-wise* photo feature \mathbf{p}_s . Bilinear upscaling, followed by *differentiable* Sigmoid thresholding yields *patch-wise* correlation mask \mathcal{M} , which when multiplied with \mathcal{P} gives *masked candidate photo* $\mathcal{P}_{\text{mask}}$ (highlighted in grey). Frozen SBIR backbone \mathcal{F} enforces the input sketches to generate masks that segment *only* the foreground object (queried via \mathcal{S}) via $\mathcal{L}_{\text{SBIR}}$. $\mathcal{L}_{\text{InfoNCE}}$ between \mathbf{s} and \mathbf{p}_s enhances sketch-photo alignment. At every batch, $\mathcal{L}_{\text{unpaired}}$ ensures an *all-zero* mask for negative samples (\mathcal{N}). To avoid overfitting to a trivial *all-one* mask, we additionally regularise \mathcal{M} via \mathcal{L}_{reg} .

global textual feature and *patch-wise visual features* [57] for better text-photo *region-wise* alignment (instead of using *global* feature for both as in CLIP training [68]) required for dense pixel-level segmentation task [57]. We however exclude the textual encoder and employ CLIP’s visual encoder to extract *patch-wise* photo features and *global* query sketch feature to apply the same loss.

In particular, we consider a pre-trained CLIP [68] ViT-L/14 backbone visual feature extractor $\mathbf{V}(\cdot)$ that splits the input \mathcal{I} into T patches and extracts patch-wise features $\{\mathcal{I}_p^i\}$ and global [CLS]-token feature \mathcal{I}_{CLS} as $\mathbf{V}(\mathcal{I}) = [\mathcal{I}_p^1, \mathcal{I}_p^2, \dots, \mathcal{I}_p^T, \mathcal{I}_{\text{CLS}}] \in \mathbb{R}^{(T+1) \times d}$. For a sketch-query \mathcal{S} , we use its *global* feature representation $\mathbf{s} = \mathbf{V}_g(\mathcal{S}) \in \mathbb{R}^{1 \times d}$ using the [CLS]-token feature, while for a candidate photo \mathcal{P} , we utilise its *patch-wise* feature representation $\mathbf{p} = \mathbf{V}_p(\mathcal{P}) \in \mathbb{R}^{T \times d}$. Although \mathbf{V} is *shared* between sketch and photo, \mathbf{V}_g and \mathbf{V}_p denotes *global* and *patch-wise* feature extraction respectively. We calculate cosine similarity between \mathbf{s} and \mathbf{p} to obtain a patch-wise correlation vector $\xi \in \mathbb{R}^{T \times 1}$ with SoftMax normalisation across the patch dimension. Finally, taking the weighted sum across the patches, we obtain the sketch-query aware photo feature as $\hat{\mathbf{p}} = \sum_{i=1}^T (\xi_i \times \mathbf{p}_i)$. We perform l_2 normalisation on \mathbf{s} and $\hat{\mathbf{p}}$ followed by calculating InfoNCE between them as:

$$\mathcal{L}_{\text{InfoNCE}} = \frac{1}{2k} \sum_{i=1}^k \left(\frac{\exp(\hat{\mathbf{p}}_i \cdot \mathbf{s}_i)}{\sum_{j=1}^k \exp(\hat{\mathbf{p}}_i \cdot \mathbf{s}_j)} + \frac{\exp(\hat{\mathbf{p}}_i \cdot \mathbf{s}_i)}{\sum_{j=1}^k \exp(\hat{\mathbf{p}}_j \cdot \mathbf{s}_i)} \right) \quad (1)$$

Here, k denotes batchsize. For a photo of size $\mathbb{R}^{224 \times 224 \times 3}$, the number of patches $T=256$ for ViT-L/14 backbone. During testing, we calculate cosine similarity between *global* sketch query feature $\mathbf{s} \in \mathbb{R}^{1 \times d}$ and *patch-wise* candidate image features $\mathbf{p} \in \mathbb{R}^{256 \times d}$ to obtain the patch-wise correlation vector $\xi \in \mathbb{R}^{256 \times 1}$ that shows the degree to which

each image patch correlates to the query-concept. We apply element-wise Sigmoid on ξ and reshape its spatial tensor equivalent of size $\mathbb{R}^{16 \times 16 \times 1}$ followed by bilinearly upscaling it to the original photo size, to get the similarity map of size $\mathbb{R}^{h \times w \times 1}$. Empirically thresholding it with a fixed value (0.5) we get the predicted binary segmentation mask.

However, this baseline suffers a few drawbacks – (i) while CLIP [68] works reasonably well on category-level tasks [72], it has limited fine-grained potential [72]. Consequently, for the fine-grained setup, we use a pre-trained DINOv2 [60] ViT-L/14 backbone which showcases better fine-grained cross-modal correspondence [60], and (ii) CLIP’s contrastive learning happens in the *embedding-space* [68], while segmentation is a *pixel-level* task. Furthermore, alignment in the latent embedding-space does not guarantee pixel-level semantic alignment. While this embedding-space alignment works well in case of *semantic-driven* text-based segmentation [57], sketches being more *shape-driven* [6, 18, 58, 72] perform sub-optimally in this case.

4.3. Sketch-guided Mask Generation

Given a sketch and a candidate image, we extract the *global* sketch-query feature $\mathbf{s} = \mathbf{V}_g(\mathcal{S}) \in \mathbb{R}^{1 \times d}$ and *patch-wise* candidate image features $\mathbf{p} = \mathbf{V}_p(\mathcal{P}) \in \mathbb{R}^{T \times d}$. We reshape (for brevity) the *patch-wise* features \mathbf{p} in the equivalent image-space spatial order to get the $\mathbf{p}_s = \text{Reshape}(\mathbf{p}) \in \mathbb{R}^{h \times w \times d}$ spatial tensor where $T = h' \times w'$. We get the *sketch-guided correlation map* \mathcal{C} by computing cosine similarity between \mathbf{s} and \mathbf{p}_s using the sketch as a *probe-vector* as:

$$\mathcal{C}(u, v) = \frac{\langle \mathbf{s}, \mathbf{p}_s(u, v) \rangle}{\|\mathbf{s}\| \|\mathbf{p}_s(u, v)\|} \quad u = [1, \dots, h'], v = [1, \dots, w'] \quad (2)$$

Now the research question remains as to how can we leverage this sketch-guided correlation map \mathcal{C} in the learning process while backpropagating the training signal via pixel space. One solution could be to bilinearly upscale $\mathcal{C} \in \mathbb{R}^{h' \times w' \times 1}$ to the original photo resolution ($\mathbb{R}^{h \times w \times 1}$), and threshold it with a fixed value and multiply with the candidate photo to get a *masked photo*, where ideally the foreground objects (w.r.t. the sketch concept) would remain *unmasked* and the background regions would be *suppressed*. Nonetheless, hard thresholding with a fixed value invokes *non-differentiability* due to the involvement of a Heaviside function [12]. To alleviate this issue, we approximate the Heaviside thresholding [12] operation with a temperature (τ) controlled Sigmoid function [12, 64] as:

$$\mathcal{M} = 1 / (1 + \exp((\mathcal{C} - 0.5) / \tau)) \quad (3)$$

where τ is the temperature parameter defining the sharpness of the Sigmoid, and 0.5 is the thresholding value. With the thresholded patch-wise correlation mask \mathcal{M} , we generate the masked candidate photo via spatial-wise multiplication as $\mathcal{P}_{\text{mask}} = \mathcal{P} \times \mathcal{M}$. During training, we aim to jointly optimise the visual encoder such that the mask generates *true* responses, *only* in those spatial regions of the

photo that contain the object drawn in the input *sketch*. Now, to quantify the quality of the masked photo in terms of *background-foreground separation*, we use a pre-trained SBIR [71] model-based loss described in the next section.

4.4. Training Objectives

Pre-trained SBIR Loss. We hypothesise that the masked photo $\mathcal{P}_{\text{mask}}$ and the query sketch \mathcal{S} will lie very close in the pre-trained SBIR model’s (\mathcal{F}) embedding space when the generated mask \mathcal{M} would *only* segment the foreground object related to the sketch query. However, when the generated mask falsely suppresses the foreground object, $\mathcal{P}_{\text{mask}}$ would likely diverge from \mathcal{S} , in the same space. Therefore, \mathcal{F} is used as a *critique* that would provide a training signal to \mathbf{V} to generate accurate foreground masks that would place $\mathcal{P}_{\text{mask}}$ and \mathcal{S} in close proximity in the latent space; otherwise a high loss is imposed. Given a distance function $\delta(\cdot, \cdot)$ the SBIR loss becomes:

$$\mathcal{L}_{\text{SBIR}} = \delta(\mathcal{F}(\mathcal{P}_{\text{mask}}), \mathcal{F}(\mathcal{S})) \quad (4)$$

Notably, for category-level and fine-grained segmentation, we use pre-trained category-level and fine-grained SBIR models [71] respectively.

Unpaired Sketch-Photo Loss. Apart from paired sketch-photo data, we focus on *unpaired* photos to ensure that *nothing* is segmented (correlation map contains only 0s) from them, as they do *not* contain the sketched query concept. We implement this via unpaired sketch-photo loss, where, across each batch, for every query-sketch \mathcal{S} , we sample a random non-paired image \mathcal{N} (from different instances for fine-grained, and different classes for category-level). We compute and reshape the *patch-wise* features of \mathcal{N} as $\mathbf{n}_s = \mathbf{V}_p(\mathcal{N}) \in \mathbb{R}^{h \times w \times d}$ and calculate cosine similarity between \mathbf{n}_s and \mathbf{s} , followed by Sigmoid normalisation to generate the correlation map \mathcal{C}_n . The model is constrained to predict an *all-zero* \mathcal{C}_n for random non-paired candidate images via a binary cross-entropy loss as:

$$\mathcal{L}_{\text{unpaired}} = -\frac{1}{h'w'} \sum_{i=1}^h \sum_{j=1}^w \log(1 - \mathcal{C}_n(i, j)) \quad (5)$$

Mask Regularisation Loss. Ideally, we want to segment *only* the foreground sketch query concept suppressing the background pixels. Nonetheless, minimising $\mathcal{L}_{\text{SBIR}}$ might result in a trivial solution of classifying *all* pixels as foreground object [89]. To eliminate the chance of a trivial mask with *all* 1s, we utilise a regularisation loss that computes the cross-entropy between the generated mask $\mathcal{M} \in \mathbb{R}^{h \times w \times 1}$ and an all-zero mask as:

$$\mathcal{L}_{\text{reg}} = -\frac{1}{hw} \sum_{i=1}^h \sum_{j=1}^w \log(1 - \mathcal{M}(i, j)) \quad (6)$$

Thus, our overall training objective (Fig. 4) becomes $\mathcal{L}_{\text{total}} = \lambda_1 \mathcal{L}_{\text{InfoNCE}} + \lambda_2 \mathcal{L}_{\text{SBIR}} + \lambda_3 \mathcal{L}_{\text{unpaired}} + \lambda_4 \mathcal{L}_{\text{reg}}$.

4.5. Further Extension to Part-level Segmentation

Part-level segmentation aims to restrict the model to segment *only* the region corresponding to the part-level sketch query (e.g., “head” of a camel). Unfortunately, common sketch-photo datasets [73] neither hold part-level sketches, nor part-level masks. We therefore aim to model this part-level behaviour via a simple sketch augmentation trick where we synthetically split the input sketch into multiple non-overlapping portions. Specifically, we first calculate the centroid of the query sketch from its vector coordinates. Now, at every pass, we draw a straight line from the centroid with a *random* slope m_1 . Based on the number of non-overlapping portions n , we calculate the slope values (m_2, m_3, \dots, m_n) for the next lines as $m_n = m_{n-1} + \frac{360}{n}$. These n straight lines segment the sketch into n orthogonal non-overlapping parts (Fig. 5). With $n=2$ (decided empirically), we segment the query sketch \mathcal{S} into two non-overlapping parts \mathcal{S}_A and \mathcal{S}_B . Using sketch-guided mask generation procedure (Sec. 4.3), we generate the corresponding masks \mathcal{M}_A and \mathcal{M}_B . Ideally, \mathcal{M}_A and \mathcal{M}_B should only segment their corresponding regions from the candidate images in a *non-overlapping* manner, which therefore incurs a penalisation if \mathcal{M}_A and \mathcal{M}_B overlap. To do so we combine \mathcal{M}_A and \mathcal{M}_B via bit-wise XOR to get the final mask as $\mathcal{M} = \mathcal{M}_A \oplus \mathcal{M}_B$, where the *common foreground regions* should be *nullified*. Consequently, the same regions will be suppressed in the masked candidate image $\mathcal{P}_{\text{mask}} = \mathcal{P} \times \mathcal{M}$ as well. Accordingly, $\mathcal{L}_{\text{SBIR}}$ would impose a high loss, leading to better part-specific segmentation.



Figure 5. Example of our sketch-partitioning augmentation. \mathcal{S} is divided into \mathcal{S}_A and \mathcal{S}_B based on the straight lines from centroid (blue dot). Common foreground region of \mathcal{M} is bordered in red.

4.6. Discussion

For category-level segmentation, we use a pre-trained category-level SBIR model (Sec. 3) with a pre-trained CLIP [68] ViT-L/14 backbone due to its category-level generalisation potential [68]. Whereas, for fine-grained segmentation, we use a pre-trained FG-SBIR model (Sec. 3) with a pre-trained DINOv2 [60] ViT-L/14 backbone. For extension to part-level, we use the same fine-grained segmentation model with the sketch-partitioning augmentation (Sec. 4.5) applied to 50% of sketch samples in each batch.

During testing, \mathbf{V}_g and \mathbf{V}_p extract global sketch features and patch-wise candidate image features \mathbf{p}_s , using which we calculate the sketch-guided correlation map \mathcal{C} (Eq. (2)). Upscaling \mathcal{C} , followed by hard thresholding it with a fixed value of 0.5 yields the final segmentation mask \mathcal{M} , which then undergoes standard CRF [42]-based post-processing.

5. Experiments

Dataset. As our method *does not* require ground truth masks, we can utilise any standard sketch-photo dataset for training. Here, we use Sketchy [73] and Sketchy-extended [48, 73] to train our category-level and fine-grained models respectively. While Sketchy [73] holds 12,500 photos from 125 classes, each having at least 5 fine-grained paired sketches, its extended version [48] carries additional 60,652 photos from ImageNet [23].

Evaluation. We evaluate for both category-level (Sketchy-extended) and fine-grained (Sketchy) setups individually on two paradigms – (i) for *unseen set* evaluation, we train our method on 104 Sketchy classes and test on the 21 unseen classes; (ii) for *seen set* evaluation, we randomly divide the 104 seen-classes into 80:20 train:test splits across samples. To evaluate segmentation accuracy, we manually annotate each test image from the Sketchy dataset with segmentation label masks to form the SketchySegment dataset. For further research, we open-sourced the SketchySegment dataset (cf. § Supplementary). Notably, our training pipeline *does not* involve any ground truth masks. Following standard literature [57, 85, 96], we use mean intersection over union (mIoU), and per-pixel classification accuracy (pAcc.) as our primary evaluation metrics for both seen and unseen sets. Additionally, we also report the harmonic mean IoU (hIoU) among the unseen and seen sets.

Implementation Details. We use a pre-trained ViT-L/14 CLIP [68] and ViT-L/14 DINOv2 [60] backbone for category-level and fine-grained segmentation models respectively. We fine-tune the LayerNorm layers of the CLIP visual encoder with a learning rate of 10^{-5} , keeping the rest of the parameters frozen. The DINOv2 encoder is fine-tuned with a low learning rate of 10^{-6} . We train the model for 200 epochs, in an NVIDIA RTX 2080-Ti GPU using AdamW [50] optimiser and a batch size of 16. All λ values are set to 1, empirically. We use pre-trained baseline SBIR and FG-SBIR models from [71].

Competitors. Due to the unavailability of sketch-based image segmentation frameworks, we compare our method with a few self-designed baselines and some naively adopted SOTAs [85, 91]. (i) *Sketch-based Baselines*: • **S-B1** is the same as our baseline weakly supervised segmentation method described in Sec. 4.2. • **S-B2** omits the unpaired Sketch-Photo Loss $\mathcal{L}_{\text{unpaired}}$, keeping the rest of the model same as ours. • **S-B3** excludes the mask regularisation loss \mathcal{L}_{reg} , keeping the rest of the model intact. (ii) *Text-based Baseline*: • **T-B1** To compare the efficacy of our sketch-based framework with conventional text-based segmenter, we design **T-B1**, following architecture of SegCLIP [52] where during inference, we additionally feed the class-label as a handcrafted prompt [95] “a photo of a [CLASS]”. (iii) *Sketch-adopted SOTAs*:

Methods		Category-level				Fine-grained			
		mIoU (S)	mIoU (U)	hIoU	pAcc.	mIoU (S)	mIoU (U)	hIoU	pAcc.
Baselines	S-B1	60.5	51.8	54.7	61.5	50.7	41.8	42.5	57.8
	S-B2	67.7	55.2	60.4	69.7	51.3	46.1	47.6	61.6
	S-B3	56.2	47.6	51.2	58.8	49.1	40.9	42.7	50.5
	T-B1	66.3	56.7	57.9	70.2	50.2	42.7	43.2	61.7
Adapted SOTAs	S-PerSAM	67.7	47.6	53.2	69.9	54.2	40.6	47.1	60.6
	S-ZS-Seg	68.2	56.9	54.5	71.1	56.4	48.8	49.6	67.4
	S-Graph-Cut	56.9	46.2	50.4	56.6	44.1	36.7	39.8	47.2
	S-Sketch-a-Segmenter	68.9	57.3	56.1	72.4	57.5	49.1	51.4	68.2
Ours		70.1	61.3	59.7	76.8	66.9	56.2	52.8	74.7

Table 1. Quantitative comparison on the Sketchy-Extended [48] and Sketchy [73] for category-level and fine-grained segmentation.

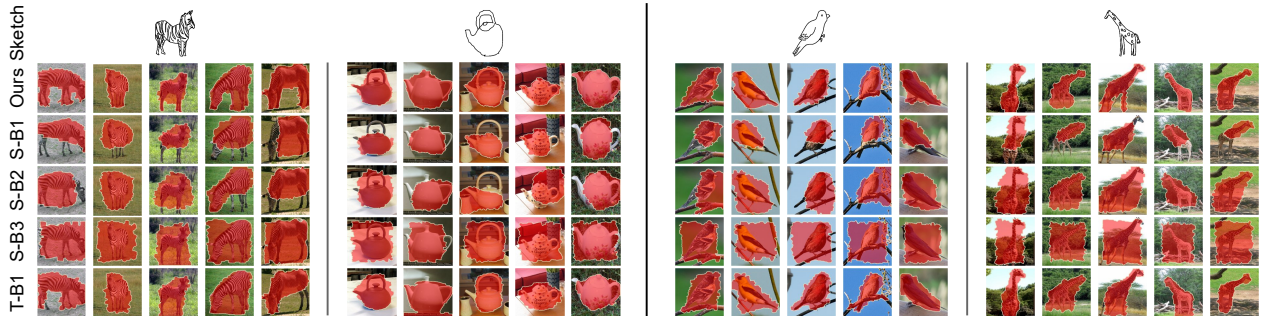


Figure 6. Qualitative comparison on Sketchy-Extended [48] for category-level segmentation on seen (left) and unseen (right) classes.

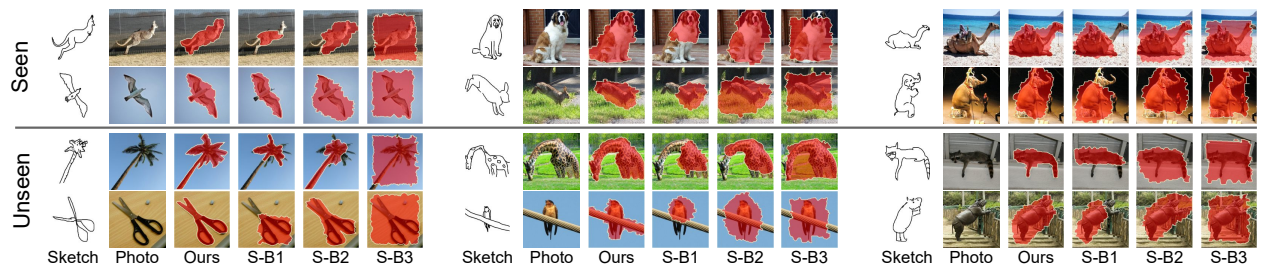


Figure 7. Qualitative comparison on Sketchy [73] for fine-grained segmentation on seen (top) and unseen (bottom) classes.

In **S-PerSAM**, given a sketch-photo pair (S, P) , we first calculate a pseudo mask ξ using our baseline segmenter (Sec. 4.2). Then, with the (ξ, P) pair, we use the pre-trained PerSAM [91] model to generate the background and foreground prompts. These prompts and candidate images upon passing through pre-trained SAM [39] yield the final segmentation masks. **S-ZS-Seg** naively adapts the two-stage text-based zero-shot segmentation framework of [85] for sketches by replacing its CLIP text encoder with a CLIP vision encoder [68] to encode input sketches. For **S-Graph-Cut**, we first generate pseudo segmentation masks using Graph-Cut [11] by using input *sketch-strokes* as the *foreground-marker*, which are then used to train a supervised CNN model [49] to generate final segmentation masks. **S-Sketch-a-Segmenter** [31] trains a DeepLabv3+-based fully-supervised segmentation model [15] and a sketch-hypernetwork [31] with *fully-annotated pixel-level masks* for each Sketchy [73] dataset images. We train/test all competitors in the same dataset/setup as ours.

5.1. Performance Analysis

Category-level Segmentation. Tab. 1 shows the following observations – (i) although **S-B2** outperforms **S-B1** (due to sub-optimal embedding-space alignment) and **S-B3** (owing to lack of mask regularisation), all these baselines fare poorly when compared to ours, particularly for **S-B3** (19.82% mIoU (S) drop vs. ours), justifying the necessity of

mask regularisation via \mathcal{L}_{reg} . (ii) **S-ZS-Seg** with its explicit zero-shot modelling [85] depicts comparable performance on both seen and unseen classes. However, **S-PerSAM** despite leveraging the large-scale pre-training of SAM [39], turns out to be sub-optimal for the unseen classes. (iii) owing to the inferior pseudo-mask generation, **S-Graph-Cut** fails to beat even the stronger baselines (*i.e.*, **S-B2**, **T-B1**). Our method outperforms these competitors with an average 8.63 (14.49)% mIoU gain on the seen (unseen) classes, even without any ground truth masks during training. Qualitative comparisons are shown in Fig. 6.

Fine-grained Segmentation. Fine-grained setup in Tab. 1 shows: (i) although **T-B1** competes ours in category-level setup, it scores a lower mIoU in the more challenging fine-grained setup. We posit that, while simple hand-crafted prompts (*i.e.*, a photo of a [CLASS]) of **T-B1** sufficed the category-level task, it failed to capture the fine-grained shape/structure. Although adding more descriptions might improve performance for **T-B1**, the research question we raise is: *how fine-grained a textual description can be? Fine-grained captions generated by SOTA captioners [43, 44] often suffer from noise and inaccuracy [43, 44]. Additionally, crafting detailed textual prompts is more laborious compared to freehand sketching [8, 10, 19].* (ii) despite being a stronger category-level baseline, **S-B2** performs sub-optimally (23.31% mIoU (S) drop vs. ours) here,

verifying the need for $\mathcal{L}_{\text{unpaired}}$ in fine-grained setting. (iii) our method outperforms all sketch-adapted SOTAs with an average hIoU margin of 13.84% without the complicated positive-negative prior calculation of **S-PerSAM**, time-consuming two-stage approach of **S-ZS-Seg**, or the allegedly unstable pseudo-mask generation of **S-Graph-Cut**. Qualitative comparisons (Fig. 7) show the fine-grained generalisation potential of our method. (iv) **S-Sketch-a-Segmenter** despite being *fully-supervised*, achieves lower hIoU and pAcc. in the Sketchy dataset.

Part-level Segmentation. Delving deeper to judge our method’s potential for part-level segmentation (*e.g.*, only the “head” of a camel), we find quantitative assessment to be infeasible, as part-level ground truth annotations are unavailable. We thus assess the part-level segmentation capability of our method qualitatively, with a set of manually edited sketches depicting a certain part of an object instance (*e.g.*, “wing” of an “airplane”). Fig. 8 shows a few images comparing the proposed method with **T-B1**. While **T-B1** often produces imprecise segmentation masks due to lingual-ambiguity of text-query [75], our method equipped with sketch-partitioning augmentation produces part-level segmentation masks that accurately captures the *semantic-intent* of end-user provided via query sketch. Furthermore, here we calculate *Mean Opinion Score (MOS)* [33] by asking 10 users to draw 25 part-level sketches and rate on a scale of 1 to 5 (bad→excellent) based on their opinion of segmentation quality. Accordingly, we obtain a higher MOS ($\mu \pm \sigma$ of 250 responses) of 4.01 ± 0.7 compared to 3.15 ± 0.2 and 3.09 ± 0.4 of **S-B1** and **T-B1** respectively.

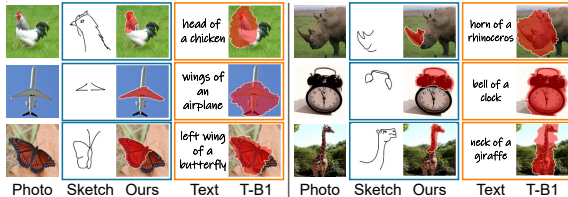


Figure 8. Part-level segmentation: **T-B1** vs. Ours on Sketchy [73].

Segmenting Composed Concepts. We also test our framework for *composed concept* segmentation. For instance, drawing a “dog” *sitting beside a “frisbee”* should segment *both* the dog and the frisbee. Qualitative comparison (on FS-COCO [58]) in Fig. 9 shows our method to perform reasonably better in segmenting composed concepts than **T-B1**.

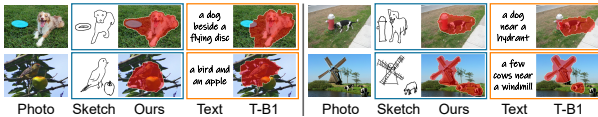


Figure 9. Composed segmentation: **T-B1** vs. Ours.

5.2. Ablation on Design

[i] Backbone Variants. Performance of our sketch-based image segmenter depends crucially on the choice of feature extractor backbone. Accordingly, we explore with multi-

ple publicly available pre-trained DINOv2 [60] and CLIP [68] backbones. Quantitative results in Sec. 5.2, show DINOv2 ViT-L/14 and CLIP ViT-L/14 to achieve the highest mIoU for fine-grained and category-level segmentation respectively. Although CLIP [68] and DINOv2 [60] show case comparable category-level performance, we posit that, due to its self-supervised pre-training, DINOv2 [60] outperforms CLIP [68] in the fine-grained setup.

[ii] Does Fine-tuning entire CLIP help? Existing literature on sketch-based vision tasks [72, 74] point towards fine-tuning the *entire* CLIP vision encoder to adapt it to their respective tasks [72, 74]. Doing so for training our category-level segmentation model however, significantly drops the final seen/unseen class mIoU (**CLIP Fine-tuning** result in Sec. 5.2). We hypothesise that fine-tuning all parameters of the vision encoder distorts the pre-trained knowledge of CLIP, thus sacrificing its generalisation potential.

[iii] Effect of $\mathcal{L}_{\text{InfoNCE}}$. We posit that the InfoNCE loss aids in proper alignment of sketch-photo features to generate accurate patch-wise correlation maps. Hence, a drop of 12.69 (17.48)% seen-class mIoU in **w/o $\mathcal{L}_{\text{InfoNCE}}$** (Sec. 5.2), for category-level (fine-grained) setup, verifies its importance in learning patch-wise sketch-photo region alignment.

[iv] Why Sketch-Partitioning Augmentation? Quantitative assessment of sketch-partitioning for part-level segmentation is infeasible due to the lack of annotation masks. However **w/o Sketch-partitioning** results in Sec. 5.2 shows our part-level augmentation to be particularly helpful for our fine-grained segmentation model, as its absence further reduces the seen (unseen) class mIoU by 8.22 (10.32)%.

Methods	Category-level		Fine-grained		
	mIoU (S)	mIoU (U)	mIoU (S)	mIoU (U)	
DINOv2	ViT-S/14	58.7	50.9	60.4	50.3
	ViT-B/14	65.1	57.2	63.6	51.7
	ViT-L/14	68.5	59.8	66.9	56.2
CLIP	ViT-B/16	59.7	51.2	54.6	43.3
	ViT-B/32	66.4	59.9	56.4	44.8
	ViT-L/14	70.1	61.3	60.1	49.7
w/o $\mathcal{L}_{\text{InfoNCE}}$	61.2	52.8	55.2	48.1	
w/o Sketch-partitioning	69.3	60.1	61.4	50.4	
CLIP Fine-tuning	60.6	32.7	–	–	
Ours-full	70.1	61.3	66.9	56.2	

Table 2. Ablation on design.

5.3. Limitations and Failure Cases

Although our method is quite robust against deformed sketches and hard-to-segment candidate images (Fig. 6-9), it sometimes struggles to yield accurate segmentation masks in case of challenging candidate images (Fig. 10) with reflection, cluttered background, occlusion, or camouflage.

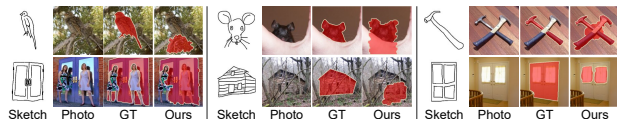


Figure 10. Failure cases. (*Best view when zoomed in.*)

6. Conclusion

Here, we explore the potential of freehand abstract sketches for *subjective* image segmentation. Leveraging large-scale pre-trained visual encoders and SBIR models, we devise a *mask-free* image segmenter that allows for segmentation at multiple granularity levels (*i.e.*, category-level and fine-grained). Furthermore, using the smart augmentation trick of sketch-partitioning, we extend our method to part-level segmentation. Extensive qualitative and quantitative results depict the efficacy of our method. We hope that this study paves the path for more sketch-based vision tasks in future.

References

- [1] Rameen Abdal, Peihao Zhu, Niloy J Mitra, and Peter Wonka. Labels4Free: Unsupervised Segmentation Using StyleGAN. In *CVPR*, 2021. 3
- [2] Ejaz Ahmed, Scott Cohen, and Brian Price. Semantic Object Selection. In *CVPR*, 2014. 3, 4
- [3] Relja Arandjelovic and Andrew Zisserman. Object Discovery with a Copy-Pasting GAN. *arXiv preprint arXiv:1905.11369*, 2019. 3
- [4] Nikita Araslanov and Stefan Roth. Single-Stage Semantic Segmentation From Image Labels. In *CVPR*, 2020. 3
- [5] Amy Bearman, Olga Russakovsky, Vittorio Ferrari, and Li Fei-Fei. What’s the Point: Semantic Segmentation with Point Supervision. In *ECCV*, 2016. 3, 4
- [6] Ayan Kumar Bhunia, Yongxin Yang, Timothy M Hospedales, Tao Xiang, and Yi-Zhe Song. Sketch Less for More: On-the-Fly Fine-Grained Sketch Based Image Retrieval. In *CVPR*, 2020. 2, 5
- [7] Ayan Kumar Bhunia, Pinaki Nath Chowdhury, Aneeshan Sain, Yongxin Yang, Tao Xiang, and Yi-Zhe Song. More Photos are All You Need: Semi-Supervised Learning for Fine-Grained Sketch Based Image Retrieval. In *CVPR*, 2021. 2
- [8] Ayan Kumar Bhunia, Viswanatha Reddy Gajjala, Subhadeep Koley, Rohit Kundu, Aneeshan Sain, Tao Xiang, and Yi-Zhe Song. Doodle It Yourself: Class Incremental Learning by Drawing a Few Sketches. In *CVPR*, 2022. 2, 7
- [9] Ayan Kumar Bhunia, Aneeshan Sain, Parth Shah, Animesh Gupta, Pinaki Nath Chowdhury, Tao Xiang, and Yi-Zhe Song. Adaptive Fine-Grained Sketch-Based Image Retrieval. In *ECCV*, 2022. 3
- [10] Ayan Kumar Bhunia, Subhadeep Koley, Amandeep Kumar, Aneeshan Sain, Pinaki Nath Chowdhury, Tao Xiang, and Yi-Zhe Song. Sketch2Saliency: Learning to Detect Salient Objects from Human Drawings. In *CVPR*, 2023. 2, 4, 7
- [11] Yuri Boykov and Gareth Funka-Lea. Graph Cuts and Efficient N-D Image Segmentation. *IJCV*, 2006. 7
- [12] Honglie Chen, Weidi Xie, Triantafyllos Afouras, Arsha Nagrani, Andrea Vedaldi, and Andrew Zisserman. Localizing Visual Sounds the Hard Way. In *CVPR*, 2021. 5
- [13] Liyi Chen, Weiwei Wu, Chenchen Fu, Xiao Han, and Yuntao Zhang. Weakly Supervised Semantic Segmentation with Boundary Exploration. In *ECCV*, 2020. 3
- [14] Liang-Chieh Chen, George Papandreou, Iasonas Kokkinos, Kevin Murphy, and Alan L. Yuille. DeepLab: Semantic Image Segmentation with Deep Convolutional Nets, Atrous Convolution, and Fully Connected CRFs. *IEEE-TPAMI*, 2017. 2, 3
- [15] Liang-Chieh Chen, Yukun Zhu, George Papandreou, Florian Schroff, and Hartwig Adam. Encoder-Decoder with Atrous Separable Convolution for Semantic Image Segmentation. In *ECCV*, 2018. 2, 3, 7
- [16] Mickael Chen, Thierry Artières, and Ludovic Denoyer. Unsupervised Object Segmentation by Redrawing. In *NeurIPS*, 2019. 3
- [17] Xi Chen, Zhiyan Zhao, Feiwu Yu, Yilei Zhang, and Manni Duan. Conditional Diffusion for Interactive Segmentation. In *ICCV*, 2021. 1
- [18] Pinaki Nath Chowdhury, Ayan Kumar Bhunia, Aneeshan Sain, Subhadeep Koley, Tao Xiang, and Yi-Zhe Song. SceneTrilogy: On Human Scene-Sketch and its Complementarity with Photo and Text. In *CVPR*, 2023. 5
- [19] Pinaki Nath Chowdhury, Ayan Kumar Bhunia, Aneeshan Sain, Subhadeep Koley, Tao Xiang, and Yi-Zhe Song. What Can Human Sketches Do for Object Detection? In *CVPR*, 2023. 2, 4, 7
- [20] John Collomosse, Tu Bui, and Hailin Jin. LiveSketch: Query perturbations for guided sketch-based visual search. In *CVPR*, 2019. 2, 3
- [21] Jifeng Dai, Kaiming He, and Jian Sun. BoxSup: Exploiting Bounding Boxes to Supervise Convolutional Networks for Semantic Segmentation. In *ICCV*, 2015. 3
- [22] Ayan Das, Yongxin Yang, Timothy Hospedales, Tao Xiang, and Yi-Zhe Song. SketchODE: Learning neural sketch representation in continuous time. In *ICLR*, 2021. 2
- [23] Jia Deng, Wei Dong, Richard Socher, Li-Jia Li, Kai Li, and Li Fei-Fei. Imagenet: A large-scale hierarchical image database. In *CVPR*, 2009. 6
- [24] Sounak Dey, Pau Riba, Anjan Dutta, Josep Lladós, and Yi-Zhe Song. Doodle to Search: Practical Zero-Shot Sketch-based Image Retrieval. In *CVPR*, 2019. 2
- [25] Anjan Dutta and Zeynep Akata. Semantically Tied Paired Cycle Consistency for Zero-Shot Sketch-based Image Retrieval. In *CVPR*, 2019. 2
- [26] Mathias Eitz, James Hays, and Marc Alexa. How do humans sketch objects? *ACM TOG*, 2012. 3
- [27] David Ha and Douglas Eck. A Neural Representation of Sketch Drawings. *ICLR*, 2018. 3
- [28] Yuying Hao, Yi Liu, Zewu Wu, Lin Han, Yizhou Chen, Guowei Chen, Lutao Chu, Shiyu Tang, Zhiliang Yu, Zeyu Chen, et al. EdgeFlow: Achieving Practical Interactive Segmentation with Edge-Guided Flow. In *ICCV*, 2021. 1
- [29] Kaiming He, Georgia Gkioxari, Piotr Dollar, and Ross Girshick. Mask R-CNN. In *ICCV*, 2017. 3
- [30] Aaron Hertzmann. Why Do Line Drawings Work? A Realism Hypothesis. *Perception*, 2020. 2
- [31] Conghui Hu, Da Li, Yongxin Yang, Timothy M Hospedales, and Yi-Zhe Song. Sketch-a-Segmenter: Sketch-based Photo Segmenter Generation. *IEEE TIP*, 2020. 2, 7

- [32] Wei-Chih Hung, Varun Jampani, Sifei Liu, Pavlo Molchanov, Ming-Hsuan Yang, and Jan Kautz. SCOPS: Self-Supervised Co-Part Segmentation. In *CVPR*, 2019. 4
- [33] Quan Huynh-Thu, Marie-Neige Garcia, Filippo Speranza, Philip Corriveau, and Alexander Raake. Study of Rating Scales for Subjective Quality Assessment of High-Definition Video. *IEEE TBC*, 2010. 8
- [34] J. Hwang, S. Yu, J. Shi, M. Collins, T. Yang, X. Zhang, and L. Chen. SegSort: Segmentation by Discriminative Sorting of Segments. In *ICCV*, 2019. 3
- [35] Jaedong Hwang, Seoung Wug Oh, Joon-Young Lee, and Bohyung Han. Exemplar-Based Open-Set Panoptic Segmentation Network. In *CVPR*, 2021. 3
- [36] Tero Karras, Samuli Laine, and Timo Aila. A Style-Based Generator Architecture for Generative Adversarial Networks. In *CVPR*, 2019. 3
- [37] Lei Ke, Mingqiao Ye, Martin Danelljan, Yifan Liu, Yu-Wing Tai, Chi-Keung Tang, and Fisher Yu. Segment Anything in High Quality. *arXiv preprint arXiv:2306.01567*, 2023. 3
- [38] Anna Khoreva, Rodrigo Benenson, Jan Hosang, Matthias Hein, and Bernt Schiele. Simple Does It: Weakly Supervised Instance and Semantic Segmentation. In *CVPR*, 2017. 3
- [39] Alexander Kirillov, Eric Mintun, Nikhila Ravi, Hanzi Mao, Chloe Rolland, Laura Gustafson, Tete Xiao, Spencer Whitehead, Alexander C Berg, Wan-Yen Lo, et al. Segment Anything. In *ICCV*, 2023. 1, 2, 3, 7
- [40] Kazuma Kobayashi, Lin Gu, Ryuichiro Hataya, Takaaki Mizuno, Mototaka Miyake, Hirokazu Watanabe, Masamichi Takahashi, Yasuyuki Takamizawa, Yukihiro Yoshida, Satoshi Nakamura, et al. Sketch-based Medical Image Retrieval. *arXiv preprint arXiv:2303.03633*, 2023. 2
- [41] Subhadeep Koley, Ayan Kumar Bhunia, Aneeshan Sain, Pinaki Nath Chowdhury, Tao Xiang, and Yi-Zhe Song. Picture that Sketch: Photorealistic Image Generation from Abstract Sketches. In *CVPR*, 2023. 2, 4
- [42] Philipp Krähenbühl and Vladlen Koltun. Efficient Inference in Fully Connected CRFs with Gaussian Edge Potentials. In *NeurIPS*, 2011. 6
- [43] Junnan Li, Dongxu Li, Caiming Xiong, and Steven Hoi. BLIP: Bootstrapping language-image pre-training for unified vision-language understanding and generation. In *ICML*, 2022. 7
- [44] Junnan Li, Dongxu Li, Silvio Savarese, and Steven Hoi. BLIP-2: Bootstrapping Language-Image Pre-training with Frozen Image Encoders and Large Language Models. In *ICML*, 2023. 7
- [45] Kungpeng Li, Ziyang Wu, Kuan-Chuan Peng, Jan Ernst, and Yun Fu. Tell Me Where to Look: Guided Attention Inference Network. In *CVPR*, 2018. 3
- [46] Di Lin, Jifeng Dai, Jiaya Jia, Kaiming He, and Jian Sun. ScribbleSup: Scribble-Supervised Convolutional Networks for Semantic Segmentation. In *CVPR*, 2016. 3
- [47] Gao Lin, Liu Feng-Lin, Chen Shu-Yu, Jiang Kaiwen, Li Chunpeng, Yukun Lai, and Fu Hongbo. SketchFaceNeRF: Sketch-based facial generation and editing in neural radiance fields. *ACM TOG*, 2023. 2
- [48] Li Liu, Fumin Shen, Yuming Shen, Xianglong Liu, and Ling Shao. Deep Sketch Hashing: Fast Free-hand Sketch-Based Image Retrieval. In *CVPR*, 2017. 3, 4, 6, 7
- [49] Jonathan Long, Evan Shelhamer, and Trevor Darrell. Fully Convolutional Networks for Semantic Segmentation. In *CVPR*, 2015. 1, 2, 3, 7
- [50] Ilya Loshchilov and Frank Hutter. Decoupled weight decay regularization. In *ICLR*, 2019. 6
- [51] Timo Lüddecke and Alexander Ecker. Image Segmentation Using Text and Image Prompts. In *CVPR*, 2022. 1
- [52] Huaishao Luo, Junwei Bao, Youzheng Wu, Xiaodong He, and Tianrui Li. SegCLIP: Patch Aggregation with Learnable Centers for Open-Vocabulary Semantic Segmentation. In *ICML*, 2023. 3, 6
- [53] Ling Luo, Yulia Gryaditskaya, Yongxin Yang, Tao Xiang, and Yi-Zhe Song. Towards 3D VR-Sketch to 3D Shape Retrieval. In *3DV*, 2020. 2
- [54] Ling Luo, Yulia Gryaditskaya, Tao Xiang, and Yi-Zhe Song. Structure-Aware 3D VR Sketch to 3D Shape Retrieval. In *3DV*, 2022. 2
- [55] Luke Melas-Kyriazi, Christian Rupprecht, Iro Laina, and Andrea Vedaldi. Finding an Unsupervised Image Segmenter in each of your Deep Generative Models. In *ICLR*, 2022. 3
- [56] Aryan Mikaeili, Or Perel, Daniel Cohen-Or, and Ali Mahdavi-Amiri. SKED: Sketch-guided Text-based 3D Editing. In *CVPR*, 2023. 2
- [57] Jishnu Mukhoti, Tsung-Yu Lin, Omid Poursaeed, Rui Wang, Ashish Shah, Philip HS Torr, and Ser-Nam Lim. Open Vocabulary Semantic Segmentation with Patch Aligned Contrastive Learning. In *CVPR*, 2023. 2, 4, 5, 6
- [58] Pinaki Nath Chowdhury, Aneeshan Sain, Yulia Gryaditskaya, Ayan Kumar Bhunia, Tao Xiang, and Yi-Zhe Song. FS-COCO: Towards Understanding of Freehand Sketches of Common Objects in Context. In *ECCV*, 2022. 2, 5, 8
- [59] Seong Joon Oh, Rodrigo Benenson, Anna Khoreva, Zeynep Akata, Mario Fritz, and Bernt Schiele. Exploiting saliency for object segmentation from image level labels. In *CVPR*, 2017. 3
- [60] Maxime Oquab, Timothée Darcet, Théo Moutakanni, Huy Vo, Marc Szafraniec, Vasil Khalidov, Pierre Fernandez, Daniel Haziza, Francisco Massa, Alaaeldin El-Nouby, et al. DINOv2: Learning Robust Visual Features without Supervision. *arXiv preprint arXiv:2304.07193*, 2023. 2, 5, 6, 8
- [61] Daniil Pakhomov, Sanchit Hira, Narayani Wagle, Kemar E Green, and Nassir Navab. Segmentation in Style: Unsupervised Semantic Image Segmentation with Stylegan and CLIP. *arXiv preprint arXiv:2107.12518*, 2021. 3
- [62] Dim P Papadopoulos, Alasdair DF Clarke, Frank Keller, and Vittorio Ferrari. Training Object Class Detectors from Eye Tracking Data. In *ECCV*, 2014. 3
- [63] George Papandreou, Liang-Chieh Chen, Kevin P Murphy, and Alan L Yuille. Weakly- and Semi-Supervised Learning of a Deep Convolutional Network for Semantic Image Segmentation. In *ICCV*, 2015. 3
- [64] Yash Patel, Giorgos Tolias, and Jiří Matas. Recall@k: Surrogate Loss with Large Batches and Similarity Mixup. In *CVPR*, 2022. 5

- [65] Deepak Pathak, Philipp Krahenbuhl, and Trevor Darrell. Constrained Convolutional Neural Networks for Weakly Supervised Segmentation. In *ICCV*, 2015. 3
- [66] Deepak Pathak, Evan Shelhamer, Jonathan Long, and Trevor Darrell. Fully Convolutional Multi-Class Multiple Instance Learning. In *ICLR*, 2015. 3
- [67] Pedro O Pinheiro and Ronan Collobert. From Image-level to Pixel-level Labeling with Convolutional Networks. In *CVPR*, 2015. 3
- [68] Alec Radford, Jong Wook Kim, Chris Hallacy, Aditya Ramesh, Gabriel Goh, Sandhini Agarwal, Girish Sastry, Amanda Askell, Pamela Mishkin, Jack Clark, et al. Learning Transferable Visual Models From Natural Language Supervision. In *ICML*, 2021. 2, 3, 4, 5, 6, 7, 8
- [69] Robin Rombach, Andreas Blattmann, Dominik Lorenz, Patrick Esser, and Björn Ommer. High-Resolution Image Synthesis with Latent Diffusion Models. In *CVPR*, 2022. 3
- [70] Olaf Ronneberger, Philipp Fischer, and Thomas Brox. U-Net: Convolutional Networks for Biomedical Image Segmentation. In *MICCAI*, 2015. 2
- [71] Aneeshan Sain, Ayan Kumar Bhunia, Yongxin Yang, Tao Xiang, and Yi-Zhe Song. StyleMeUp: Towards Style-Agnostic Sketch-Based Image Retrieval. In *CVPR*, 2021. 3, 5, 6
- [72] Aneeshan Sain, Ayan Kumar Bhunia, Pinaki Nath Chowdhury, Subhadeep Koley, Tao Xiang, and Yi-Zhe Song. CLIP for All Things Zero-Shot Sketch-Based Image Retrieval, Fine-Grained or Not. In *CVPR*, 2023. 2, 3, 4, 5, 8
- [73] Patsorn Sangkloy, Nathan Burnell, Cusuh Ham, and James Hays. The Sketchy Database: Learning to Retrieve Badly Drawn Bunnies. *ACM TOG*, 2016. 2, 3, 4, 6, 7, 8
- [74] Patsorn Sangkloy, Wittawat Jitkrittum, Diyi Yang, and James Hays. A Sketch Is Worth a Thousand Words: Image Retrieval with Text and Sketch. In *ECCV*, 2022. 2, 8
- [75] Idan Schwartz, Vésteinn Snæbjarnarson, Hila Chefer, Serge Belongie, Lior Wolf, and Sagie Benaim. Discriminative Class Tokens for Text-to-Image Diffusion Models. In *ICCV*, 2023. 8
- [76] RR Selvaraju, M Cogswell, A Das, R Vedantam, D Parikh, and D Batra. Grad-CAM: Visual Explanations from Deep Networks via Gradient-based Localization. In *ICCV*, 2017. 3
- [77] Zhi Tian, Chunhua Shen, and Hao Chen. Conditional Convolutions for Instance Segmentation. In *ECCV*, 2020. 3
- [78] Wouter Van Gansbeke, Simon Vandenhende, Stamatios Georgoulis, and Luc Van Gool. Unsupervised Semantic Segmentation by Contrasting Object Mask Proposals. In *ICCV*, 2021. 3
- [79] Paul Vernaza and Manmohan Chandraker. Learning random-walk label propagation for weakly-supervised semantic segmentation. In *CVPR*, 2017. 3
- [80] Andrey Voynov, Stanislav Morozov, and Artem Babenko. Object Segmentation Without Labels with Large-Scale Generative Models. In *ICML*, 2022. 3
- [81] Enze Xie, Wenhai Wang, Alan L. Yuille, Anima Anandkumar, and Jose M. Alvarez. SegFormer: Simple and Efficient Design for Semantic Segmentation with Transformers. In *CVPR*, 2021. 2
- [82] Zhengyang Xie, Zhuang Liu, Eduard Hovy, Liangzhe Yuan, and Veselin Stoyanov. Invariant Information Clustering for Unsupervised Image Classification and Segmentation. In *ICCV*, 2019. 3
- [83] Jiarui Xu, Shalini De Mello, Sifei Liu, Wonmin Byeon, Thomas Breuel, Jan Kautz, and Xiaolong Wang. GroupViT: Semantic Segmentation Emerges from Text Supervision. In *CVPR*, 2022. 3
- [84] Jiarui Xu, Sifei Liu, Arash Vahdat, Wonmin Byeon, Xiaolong Wang, and Shalini De Mello. Open-Vocabulary Panoptic Segmentation with Text-to-Image Diffusion Models. In *CVPR*, 2023. 3
- [85] Mengde Xu, Zheng Zhang, Fangyun Wei, Yutong Lin, Yue Cao, Han Hu, and Xiang Bai. A Simple Baseline for Open-Vocabulary Semantic Segmentation with Pre-trained Vision-language Model. In *ECCV*, 2022. 2, 6, 7
- [86] Sasi Kiran Yelamarthi, Shiva Krishna Reddy, Ashish Mishra, and Anurag Mittal. A Zero-Shot Framework for Sketch Based Image Retrieval. In *ECCV*, 2018. 2
- [87] Jiahui Yu, Zhe Lin, Jimei Yang, Xiaohui Shen, Xin Lu, and Thomas S Huang. Free-Form Image Inpainting with Gated Convolution. In *ICCV*, 2019. 2
- [88] Qian Yu, Feng Liu, Yi-Zhe Song, Tao Xiang, Timothy M Hospedales, and Chen-Change Loy. Sketch Me That Shoe. In *CVPR*, 2016. 3
- [89] Yu Zeng, Yunzhi Zhuge, Huchuan Lu, Lihe Zhang, Mingyang Qian, and Yizhou Yu. Multi-source weak supervision for saliency detection. In *CVPR*, 2019. 5
- [90] Yu Zeng, Zhe Lin, and Vishal M Patel. SketchEdit: Mask-Free Local Image Manipulation with Partial Sketches. In *CVPR*, 2022. 2
- [91] Renrui Zhang, Zhengkai Jiang, Ziyu Guo, Shilin Yan, Junting Pan, Hao Dong, Peng Gao, and Hongsheng Li. Personalize Segment Anything Model with One Shot. In *ICLR*, 2024. 1, 3, 6, 7
- [92] Xiao Zhang and Michael Maire. Self-Supervised Visual Representation Learning from Hierarchical Grouping. In *NeurIPS*, 2020. 3
- [93] Sixiao Zheng, Jiachen Lu, Hengshuang Zhao, Xiatian Zhu, Zekun Luo, Yabiao Wang, Yanwei Fu, Jianfeng Feng, Tao Xiang, Philip H. S. Torr, and Li Zhang. Rethinking Semantic Segmentation from a Sequence-to-Sequence Perspective with Transformers. In *CVPR*, 2021. 2
- [94] Bolei Zhou, Aditya Khosla, Agata Lapedriza, Aude Oliva, and Antonio Torralba. Learning Deep Features for Discriminative Localization. In *CVPR*, 2016. 3
- [95] Kaiyang Zhou, Jingkang Yang, Chen Change Loy, and Ziwei Liu. Learning to Prompt for Vision-Language Models. *IJCV*, 2022. 6
- [96] Ziqin Zhou, Yinjie Lei, Bowen Zhang, Lingqiao Liu, and Yifan Liu. ZegCLIP: Towards Adapting CLIP for Zero-shot Semantic Segmentation. In *CVPR*, 2023. 6